Stronger and weaker singularity of an inclined crack terminating at the orthotropic bimaterial interface

Tomáš Profant[1, a], Michal Kotoul[1,b] and Oldřich Ševeček[1,c]

[1] Institute of Solid Mechanics, Mechatronics and Biomechanics, Faculty of Mechanical Engineering, Brno University of Technology, Technická 2, 616 69, Brno, Czech Republic

[a]profant@fme.vutbr.cz, [b] kotoul@fme.vutbr.cz , [c]sevecek@atlas.cz

Keywords: Inclined crack, bimaterial interface, matched asymptotic expansions, reciprocal theorem, finite element method

Abstract. The attention is focused to the development of techniques for evaluation of stress singularities and generalized stress intensity factors (GSIF) pertaining to the case of an inclined surface crack terminating at the interface between two orthotropic materials. The knowledge of the regular and auxiliary solution allows evaluating the GSIF using the reciprocal theorem (Ψ-integral). A co-operating effect of a stronger and a weaker singular stress field for a crack impinging a bimaterial interface is investigated.

Introduction

Two main approaches to crack deflection have been proposed in the literature, depending on the mechanism considered: either the main crack is supposed to reach the interface and to be lying stationary [1] or a crack is nucleated at the interface ahead of the main crack [2].

With the first approach, an arbitrary short crack extension must be introduced in the interface or in the next material for the analysis based on an energy balance. The presence of these crack extensions is required to express the conditions of extension. It is assumed that this finite crack extension is controlled by the singular field of the main crack. For an inclined crack impinging a bimaterial interface the singular field generally consists of two modes exhibiting different singularity strength – stronger and weaker singularity. Because the introduced crack extension possesses a finite length, the weaker singularity can play an important role.

The aim is to investigate a co-operating effect of a stronger and a weaker singular stress field for a crack impinging a bimaterial interface between two orthotropic materials. The impinging crack may either penetrate across, or debond the interface. The concept of matched asymptotic expansions together with the contour integral based upon reciprocal theorem becomes very useful to derive the formula for the energy release rate in terms of the crack length l, the singularity exponent δ and the generalized stress intensity factors.

Analysis of crack tip singularity

The singular stress field of inclined crack impinging a bimaterial interface between two orthotropic materials is analyzed by means of continuously distributed edge dislocations technique for semi-infinite crack. It is assumed that the principal axes of both materials are aligned and the bimaterial interface is parallel or perpendicular to the principal axes. Since both of the materials' principal axes in the out of plane direction are assumed to be parallel with the z-axis, the anti-plane deformation can be decoupled from the in-plane deformation. Two coordinate systems are introduced: the primary coordinate system x_1,x_2,x_3 aligned with the material principal axes and the coordinate system x_1',x_2',x_3 rotated around the x_3 axis with x_2' coinciding with the inclined crack. For plane deformation, the elastic field can be represented in terms of complex potential functions $\Phi_1(z_1)$, $\Phi_2(z_2)$, $\Phi_3(z_3)$, each of which is holomorphic in its arguments $z_\alpha = x_1 + p_\alpha x_2$. Here, p_α are three distinct complex numbers with positive imaginary parts, which are obtained as the roots of the characteristic equation

$$\det\left[c_{i1k1}+p\left(c_{i1k2}+c_{i2k1}\right)+p^{2}c_{i2k2}\right]=0, \tag{1}$$

where c_{ijkl} is the tensor of elastic constants. With these holomorphic functions, the representation for the displacements u_i and stresses σ_{ij} is

$$u_i=2\,\mathrm{Re}\left[\sum_{\alpha=1}^{3}A_{i\alpha}\Phi_{\alpha}\left(z_{\alpha}\right)\right],\ \ \sigma_{2i}=2\,\mathrm{Re}\left[\sum_{\alpha=1}^{3}L_{i\alpha}\Phi_{\alpha}'\left(z_{\alpha}\right)\right],\ \ \sigma_{1i}=-2\,\mathrm{Re}\left[\sum_{\alpha=1}^{3}L_{i\alpha}p_{\alpha}\Phi_{\alpha}'\left(z_{\alpha}\right)\right]. \tag{2}$$

A and **L** are matrices given by $L_{i\alpha}=A_{k\alpha}\left(c_{i2k1}+p_{\alpha}c_{i2k2}\right)$, where $A_{k\alpha}$ denotes the eigenvector corresponding to the eigenvalue p_{α} above. The matrices and potential functions are expressed in the primary coordinate system. The asymptotic stress field near the crack tip is modelled as a continuous distribution of dislocations along the x_2'axis of the coordinate system connected to the crack with density function $f_k\left(x_{2o}'\right)=Hg_k\left(-x_{2o}'\right)^{\delta-1}$, $x_{2o}'<0$, where δ is the stress singularity exponent, which is yet unknown, g_k are the components of corresponding eigenvector, and H is the generalized stress intensity factor (GSIF). The resulting eigenvalue problem can be written as follows

$$\mathbf{D}'(\delta)\mathbf{g}=0,\text{where } D_{ik}'(\delta)=\mathrm{Re}\left\{\left[\sum_{\alpha}\sum_{\beta}L_{i\alpha}'^{II}G_{\alpha\beta}'\bar{M}_{\beta k}'^{II}\left(-\frac{\bar{p}_{\beta}'^{II}}{p_{\alpha}'^{II}}\right)^{-\delta}\csc\left(\pi(1-\delta)\right)-\delta_{ik}\cot\left(\pi(1-\delta)\right)\right]\right\}, \tag{3}$$

where superscripts I and II refer to the materials I and II respectively, see Fig. 1. All matrices and eigenvalues $p_{\alpha(\beta)}$ are expressed in the rotated coordinate system connected to the crack. Specifically,

$$\begin{gathered}p_{\alpha(\beta)}'=\frac{p_{\alpha(\beta)}\cos\omega-\sin\omega}{p_{\alpha(\beta)}\sin\omega+\cos\omega},\ \mathbf{A}'=\mathbf{\Omega A},\ \mathbf{L}'=\mathbf{\Omega L},\ \mathbf{G}'=\mathbf{G}\ \text{where}\\ \mathbf{G}=-i\mathbf{M}^{II}\bar{\mathbf{H}}^{-1}\left(\bar{\mathbf{A}}^{II}\bar{\mathbf{M}}^{II}-\bar{\mathbf{A}}^{I}\bar{\mathbf{M}}^{I}\right)\bar{\mathbf{L}}^{II},\ \mathbf{H}=i\left(\mathbf{A}^{I}\mathbf{M}^{I}-\bar{\mathbf{A}}^{II}\bar{\mathbf{M}}^{II}\right),\ \mathbf{M}=\mathbf{L}^{-1},\mathbf{\Omega}=\begin{bmatrix}\cos\omega & \sin\omega\\ -\sin\omega & \cos\omega\end{bmatrix},\end{gathered} \tag{4}$$

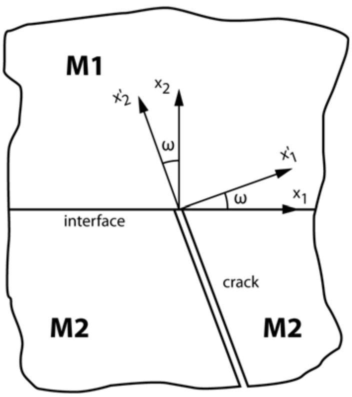

Figure 1: Scheme of inclined crack impinging a bimaterial interface

where ω is the angle formed by the crack and the interface normal. The parameter δ is calculated from the characteristic equation $\mathrm{Det}\left[\mathbf{D}'(\delta)\right]=0$ and the eigenvector **g** is determined from Eq. 3 up to a multiplicative constant. For an inclined crack impinging a bimaterial interface there exist generally two exponents of singularity: the stronger singularity exponent denoted by δ_1 and the weaker singularity exponent denoted by δ_2. The corresponding displacement fields are $r^{\delta_1}\mathbf{u}_1(\theta)$ and $r^{\delta_2}\mathbf{u}_2(\theta)$, and the generalized stress intensity factors are denoted by H_1 and H_2 respectively. It can be proved that if δ is a root of Eq. 3, then -δ also verifies this equation.

Matched asymptotic analysis

Matched asymptotic procedure [3] is used to derive the change of potential energy. Consider a perturbation of the domain Ω with crack impinging the interface; the perturbation is a deflected (double) crack extension of length a_d or penetrating crack extension of length a_p with the small perturbation parameter τ defined as $\tau = a/L \ll 1,\ a = a_p, a_d$, where L is the characteristic length of Ω. A second scale to the problem can be introduced, represented by the scaled-up coordinates $y = x/\tau$, or $(y_1, y_2) = (x_1/\tau, x_2/\tau)$ which provides a zoomed-in view into the region surrounding the crack. The displacement $\mathbf{U}^\tau$ of the perturbed elasticity problem due to the crack extension can now be expressed in terms of the regular coordinate x and the scaled-up coordinate y as $\mathbf{U}^\tau(x) = \mathbf{U}^\tau(\tau y) = \mathbf{V}^\tau(y)$, where the definition of the function $\mathbf{V}^\tau$ has been introduced, simply by a change of variable from x to y. Consider now the asymptotic expansion for $\mathbf{U}^\tau$ (which is also known as the ''outer expansion'') and for $\mathbf{V}^\tau$ (which is also known as the ''inner expansion''),

$$\mathbf{U}^\tau(x) = f_0(\tau)\mathcal{U}_0(x) + f_1(\tau)\mathcal{U}_1(x) + ... = \sum_{i=0}^{\infty} f_i(\tau)\mathcal{U}_i(x), \ \text{outer expansion}, \tag{5}$$

where $\lim_{\tau\to 0} f_{i+1}(\tau)/f_i(\tau) = 0,\ \forall i = 1,2,...$ and $\{\mathcal{U}_1, \mathcal{U}_2, ...\}$ form a set of linearly independent basis functions, and

$$\mathbf{V}^\tau(y) = F_0(\tau)\mathcal{V}_0(y) + F_1(\tau)\mathcal{V}_1(y) + ... = \sum_{i=0}^{\infty} F_i(\tau)\mathcal{V}_i(y), \ \text{inner expansion}, \tag{6}$$

where $\lim_{\tau\to 0} F_{i+1}(\tau)/F_i(\tau) = 0,\ \forall i = 1,2,...$ and $\{\mathcal{V}_1, \mathcal{V}_2, ...\}$ form a set of linearly independent basis functions. The basis functions $\{\mathcal{U}_i\}$ satisfy the elasticity problem on the same domain $\Omega \approx \Omega^\tau$ but with zero body force and with homogeneous boundary conditions. Asymptotic expansion for the primary inclined crack before the perturbation inception takes place reads

$$\mathbf{U}^0(x) = \mathbf{U}^0(0) + H_1 r^{\delta_1}\mathbf{u}_1(\theta) + H_2 r^{\delta_2}\mathbf{u}_2(\theta) + .. \tag{7}$$

The outer expansion for the perturbed domain Ω^τ is

$$\mathbf{U}^\tau(x) = \mathbf{U}^0(x) + f_1(\tau)K_{1d(p)}r^{-\delta_1}\mathbf{u}_{-1}(\theta) + f_2(\tau)K_{2d(p)}r^{-\delta_2}\mathbf{u}_{-2}(\theta) + ... \tag{8}$$

The inner expansion for the perturbed domain Ω^τ reads

$$\mathbf{V}^{\tau}(y)=F_1(\tau)\left[\rho^{\delta_1}\mathbf{u}_{1}(\theta)+K_{1d(p)}\rho^{-\delta_1}\mathbf{u}_{-1}(\theta)+K_{2d(p)}\rho^{-\delta_2}\mathbf{u}_{-2}(\theta)+...\right]+F_2(\tau)\times$$
$$\times\left[\rho^{\delta_2}\mathbf{u}_{2}(\theta)+K'_{1d(p)}\rho^{-\delta_1}\mathbf{u}_{-1}(\theta)+K'_{2d(p)}\rho^{-\delta_2}\mathbf{u}_{-2}(\theta)+....\right]+...,\quad (F_0(\tau)=1,\ \mathcal{V}_0(y)=\mathbf{U}^0(0)=0,\rho=\frac{r}{\tau}). \tag{9}$$

The first terms in the brackets on the right-hand side of Eq. 9 describe the behaviour of functions $\mathcal{V}_i$ for $\rho\rightarrow\infty$. $\mathbf{u}_{-1}(\theta),\mathbf{u}_{-2}(\theta)$ are dual solutions to $\mathbf{u}_{1}(\theta),\mathbf{u}_{2}(\theta)$, see above.

In the absence of body forces the reciprocal theorem states that the following integral is path independent

$$\Psi(\mathbf{u},\mathbf{v})=\int_{\Gamma}\left[\sigma_{kl}(\mathbf{u})n_k v_l-\sigma_{kl}(\mathbf{v})n_k u_l\right]\mathrm{d}s,\quad k,l=1,2, \tag{10}$$

where Γ is any contour surrounding the crack tip and **u**, **v** are two admissible displacement fields. If the following displacement fields are considered $\mathbf{u}=r^{\delta_i}\mathbf{u}_i(\theta)$, $\mathbf{v}=r^{\delta_j}\mathbf{u}_j(\theta)$, one can show that the contour integral Ψ is equal to zero for $\delta_i\neq-\delta_j$ and non-zero if $\delta_i=-\delta_j$. Since the basis functions corresponding to the coefficients H_1, H_2 in the asymptotic expansion for $\mathbf{U}^{\tau}$ are $r^{\delta_1}\mathbf{u}_1(\theta),r^{\delta_2}\mathbf{u}_2(\theta)$, due to the former orthogonality conditions the GSIFs H_1 and H_2 can be computed as follows:

$$H_1=\frac{\Psi\left(\mathbf{U}^{\tau},r^{-\delta_1}\mathbf{u}_{-1}\right)}{\Psi\left(r^{\delta_1}\mathbf{u}_{1},r^{-\delta_1}\mathbf{u}_{-1}\right)},\ H_2=\frac{\Psi\left(\mathbf{U}^{\tau},r^{-\delta_2}\mathbf{u}_{-2}\right)}{\Psi\left(r^{\delta_2}\mathbf{u}_{2},r^{-\delta_2}\mathbf{u}_{-2}\right)}\quad. \tag{11}$$

Since the exact solution $\mathbf{U}^{\tau}$ is not known, a finite element solution $\mathbf{U}^{h}$ can be used as an approximation for $\mathbf{U}^{\tau}$ so to obtain an approximation for H_1, H_2. The determination of the coefficients $K_{1d(p)},K_{2d(p)},K'_{1d(p)},K'_{2d(p)}$, proceeds in a similar fashion as for H_1, H_2. $K_{1d(p)},K_{2d(p)}$ are calculated in the inner domain whose remote boundary $\partial\Omega_{\text{in}}$ is subjected to the boundary condition $\mathbf{U}|_{\partial\Omega_{in}}=\rho^{\delta_1}\mathbf{u}_{1}(\theta)$

$$K_{1d(p)}=\frac{\Psi\left(\mathcal{V}_1^h(y),\rho^{\delta_1}\mathbf{u}_1\right)}{\Psi\left(\rho^{-\delta_1}\mathbf{u}_{-1},\rho^{\delta_1}\mathbf{u}_1\right)},\ K_{2d(p)}=\frac{\Psi\left(\mathcal{V}_1^h(y),\rho^{\delta_2}\mathbf{u}_2\right)}{\Psi\left(\rho^{-\delta_2}\mathbf{u}_{-2},\rho^{\delta_2}\mathbf{u}_2\right)},\ \mathcal{V}_1^h\text{-FEM approximation to }\mathbf{V}^{\tau}. \tag{12}$$

Similarly, the coefficients $K'_{1d(p)},K'_{2d(p)}$ are calculated in the inner domain whose remote boundary $\partial\Omega_{\text{in}}$ is subjected to the boundary condition $\mathbf{U}|_{\partial\Omega_{in}}=\rho^{\delta_2}\mathbf{u}_{2}(\theta)$

$$K'_{1d(p)}=\frac{\Psi\left(\mathcal{V}_2^h(y),\rho^{\delta_1}\mathbf{u}_1\right)}{\Psi\left(\rho^{-\delta_1}\mathbf{u}_{-1},\rho^{\delta_1}\mathbf{u}_1\right)},\ K'_{2d(p)}=\frac{\Psi\left(\mathcal{V}_2^h(y),\rho^{\delta_2}\mathbf{u}_2\right)}{\Psi\left(\rho^{-\delta_2}\mathbf{u}_{-2},\rho^{\delta_2}\mathbf{u}_2\right)},\ \mathcal{V}_2^h-\text{FEM approximation to }\mathbf{V}^{\tau}. \tag{13}$$

Outer and the inner asymptotic expansions read

$$\mathbf{U}^{\tau}(x=\tau y)=H_1\tau^{\delta_1}\rho^{\delta_1}\mathbf{u}_1(\theta)+H_2\tau^{\delta_2}\rho^{\delta_2}\mathbf{u}_2(\theta)+f_1(\tau)K_{1d(p)}\tau^{-\delta_1}\rho^{-\delta_1}\mathbf{u}_{-1}(\theta)+$$
$$f_2(\tau)K_{2d(p)}\tau^{-\delta_2}\rho^{-\delta_2}\mathbf{u}_{-2}(\theta)+...=\mathbf{V}^{\tau}(y)=F_1(\tau)\left[\rho^{\delta_1}\mathbf{u}_{1}(\theta)+K_{1d(p)}\rho^{-\delta_1}\mathbf{u}_{-1}(\theta)+K_{2d(p)}\rho^{-\delta_2}\mathbf{u}_{-2}(\theta)+...\right]+ \tag{14}$$
$$+F_2(\tau)\left[\rho^{\delta_2}\mathbf{u}_2(\theta)+K'_{1d(p)}\rho^{-\delta_1}\mathbf{u}_{-1}(\theta)+K'_{2d(p)}\rho^{-\delta_2}\mathbf{u}_{-2}(\theta)+....\right]+...,$$

where $f_1(\tau)$, $f_2(\tau)$, $F_1(\tau)$, $F_2(\tau)$ are found from the matching conditions:

$$\begin{aligned}
&H_1\tau^{\delta_1}\rho^{\delta_1}\mathbf{u}_1(\theta)=F_1(\tau)\rho^{\delta_1}\mathbf{u}_1(\theta)\Rightarrow F_1(\tau)=H_1\tau^{\delta_1},\\
&H_2\tau^{\delta_2}\rho^{\delta_2}\mathbf{u}_2(\theta)=F_2(\tau)\rho^{\delta_2}\mathbf{u}_2(\theta)\Rightarrow F_2(\tau)=H_2\tau^{\delta_2},\\
&f_1(\tau)K_{1d(p)}\tau^{-\delta_1}\rho^{-\delta_1}\mathbf{u}_{-1}(\theta)=F_1(\tau)K_{1d(p)}\rho^{-\delta_1}\mathbf{u}_{-1}(\theta)\Rightarrow f_1(\tau)=H\tau^{2\delta_1},\\
&F_2(\tau)K_{2d(p)}\rho^{-\delta_2}\mathbf{u}_{-2}(\theta)=f_2(\tau)K_{2d(p)}\tau^{-\delta_2}\rho^{-\delta_2}\mathbf{u}_{-2}(\theta)\Rightarrow f_2(\tau)=H_2\tau^{2\delta_2}
\end{aligned}\tag{15}$$

Finally, the inner asymptotic expansion $\mathbf{V}^\tau(y)$ follows as

$$\begin{aligned}
&\mathbf{U}^\tau(x=\tau y)=\mathbf{V}^\tau(y)=H_1\tau^{\delta_1}\left[\rho^{\delta_1}\mathbf{u}_1(\theta)+K_{1d(p)}\rho^{-\delta_1}\mathbf{u}_{-1}(\theta)+K_{2d(p)}\rho^{-\delta_2}\mathbf{u}_{-2}(\theta)+\ldots\right]+\\
&+H_2\tau^{\delta_2}\left[\rho^{\delta_2}\mathbf{u}_2(\theta)+K'_{1d(p)}\rho^{-\delta_1}\mathbf{u}_{-1}(\theta)+K'_{2d(p)}\rho^{-\delta_2}\mathbf{u}_{-2}(\theta)+\ldots.\right]+..
\end{aligned}\tag{16}$$

Incremental energy release rate and mode mixity

The incremental energy release rate (ERR) $G_{d(p)}$ is defined as

$$\begin{aligned}
&G_{d(p)}=-\frac{\delta W}{\tau_{d(p)}L}=-\frac{W^\tau-W^0}{\tau_{d(p)}L}=-\frac{1}{2\tau_{d(p)}L}\int_\Gamma\left(\sigma_{kl}\left(\mathbf{U}^\tau\right)n_kU_l^0-\sigma_{kl}\left(\mathbf{U}^0\right)n_kU_l^\tau\right)ds=-\frac{1}{2\tau_{d(p)}L}\Psi\left(\mathbf{U}^\tau,\mathbf{U}^0\right)=\\
&=-\frac{1}{2\tau_{d(p)}L}\Psi\Big(H_1\tau_{d(p)}^{\delta_1}\left[\rho^{\delta_1}\mathbf{u}_1(\theta)+K_{1d(p)}\rho^{-\delta_1}\mathbf{u}_{-1}(\theta)+K_{2d(p)}\rho^{-\delta_2}\mathbf{u}_{-2}(\theta)+..\right]+\\
&+H_2\tau_{d(p)}^{\delta_2}\left[\rho^{\delta_2}\mathbf{u}_2(\theta)+K'_{1d(p)}\rho^{-\delta_1}\mathbf{u}_{-1}(\theta)+K'_{2d(p)}\rho^{-\delta_2}\mathbf{u}_{-2}(\theta)+..\right]+..,H_1\tau_{d(p)}^{\delta_1}\rho^{\delta_1}\mathbf{u}_1(\theta)+H_2\tau_{d(p)}^{\delta_2}\rho^{\delta_2}\mathbf{u}_2(\theta)+..\Big)=\\
&=\frac{1}{2L}H_1^2K_{1d(p)}\tau_{d(p)}^{2\delta_1-1}\Psi\left(\rho^{\delta_1}\mathbf{u}_1(\theta),\rho^{-\delta_1}\mathbf{u}_{-1}(\theta)\right)+\frac{1}{2L}H_1H_2K'_{1d(p)}\tau_{d(p)}^{\delta_1+d_2-1}\Psi\left(\rho^{\delta_1}\mathbf{u}_1(\theta),\rho^{-\delta_1}\mathbf{u}_{-1}(\theta)\right)+\\
&+\frac{1}{2L}H_1H_2K_{2d(p)}\tau_{d(p)}^{\delta_1+d_2-1}\Psi\left(\rho^{\delta_2}\mathbf{u}_2(\theta),\rho^{-\delta_2}\mathbf{u}_{-2}(\theta)\right)+\frac{1}{2L}H_2^2K'_{2d(p)}\tau_{d(p)}^{2\delta_2-1}\Psi\left(\rho^{\delta_2}\mathbf{u}_2(\theta),\rho^{-\delta_2}\mathbf{u}_{-2}(\theta)\right)+..,
\end{aligned}\tag{17}$$

where $\tau_{d(p)}=a_{d(p)}/L$. Observe, that line Γ is any contour surrounding the crack tip and the crack increment and starting and finishing on the stress-free faces of he primary crack. Among others, the crack extension faces along a_p or a_d respectively, form an admissible contour which allows to rewrite Eq. 17 as a work done along $a_{d(p)}$ and leads to the classical virtual crack closure method [4]

$$\begin{aligned}
&G_{d(p)}=-\frac{\delta W}{\tau_{d(p)}L}=-\frac{W^\tau-W^0}{\tau_{d(p)}L}=-\frac{1}{2a_{d(p)}}\int_{a_{d(p)}}\left(\sigma_{kl}\left(\mathbf{U}^\tau\right)n_kU_l^0-\sigma_{kl}\left(\mathbf{U}^0\right)n_kU_l^\tau\right)ds=\\
&=\frac{1}{2a_{d(p)}}\int_{a_{d(p)}}\sigma_{kl}\left(\mathbf{U}^0\right)n_kU_l^\tau\,ds=\frac{1}{2a_{d(p)}}\int_0^{a_{d(p)}}\sigma_{kl}\left(\mathbf{U}^0\right)n_k\Delta U_l^\tau ds,
\end{aligned}\tag{18}$$

where the integral along $a_{d(p)}$ means along two faces $a_{d(p)}^+$ and $a_{d(p)}^-$ and ΔU^τ denotes $\Delta U_l^\tau=\left(U_l^\tau\right)^+-\left(U_l^\tau\right)^-$ where the sign + or – refer to upper or lower crack face. The Eq. 18 is rather difficult to handle numerically since the singularities govern the behaviour along $a_{d(p)}$. Nevertheless, it offers an idea to calculate the fracture mode mixity based upon the energy release rate (ERR). It will be discussed later.

The ratio of the debonding to the penetrating ERR follows from Eq.17 as

$$\frac{G_d}{G_p}=\frac{K_{1d}\Psi_1+\left(K'_{1d}\Psi_1+K_{2d}\Psi_2\right)\eta_d+K'_{2d}\Psi_2\eta_d^2}{K_{1p}\Psi_1+\left(K'_{1p}\Psi_1+K_{2p}\Psi_2\right)\eta_p+K'_{2p}\Psi_2\eta_p^2}\left(\frac{a_d}{a_p}\right)^{2\delta_1-1},\eta_d=\frac{H_2}{H_1}\left(\frac{a_d}{L}\right)^{\delta_2-\delta_1},\eta_p=\frac{H_2}{H_1}\left(\frac{a_p}{L}\right)^{\delta_2-\delta_1} \tag{19}$$
$$\Psi_1\equiv\Psi\left(\rho^{\delta_1}\mathbf{u}_1(\theta),\rho^{-\delta_1}\mathbf{u}_{-1}(\theta)\right),\ \ \Psi_2\equiv\Psi\left(\rho^{\delta_2}\mathbf{u}_2(\theta),\rho^{-\delta_2}\mathbf{u}_{-2}(\theta)\right),$$

which corresponds to the relation obtained by the authors [5] in a different way, see their Eq. 18. The fracture mode mixity based on the stress intensity factor (SIF) concept is usually represented by the so-called local phase angle ψ_K defined by $K=K_1+iK_2=|K|e^{i\psi_K}$ where K is the complex stress intensity factor (SIF), associated to a reference length l according to the proposal by Rice [6].

The ERR based fracture mode mixity originally results from the application of the virtual crack closure method. Consider a small but finite length a_d of a virtual crack extension along the interface. The energy release rate (ERR) associated to this crack extent is

$$G_d(a_d)=G_{dI}(a_d)+G_{dII}(a_d) \tag{20}$$

where

$$G_{dI}(a_d)=\frac{1}{2a_d}\int_0^{a_d}\sigma_{22}(s,0)\Delta u_2(a_d-s)ds,\ \ G_{dII}(a_d)=\frac{1}{2a_d}\int_0^{a_d}\sigma_{12}(s,0)\Delta u_1(a_d-s)ds \tag{21}$$

The Mode I component G_{dI} corresponds to the energy released by normal stresses acting through crack face opening displacements, and Mode II component G_{dII} corresponds to the energy released by shear stresses acting through crack face sliding displacements. The energetic mode mixity G_{dI}/G_{dII} for interface crack depends on a_d . The associated phase angle ψ_G is defined as

$$\tan^2\psi_G=\frac{G_{dII}(a_d)}{G_{dI}(a_d)} \tag{22}$$

Instead of Eq. 21, the concept of Ψ can be applied for to evaluate the phase angle ψ_G. First observe that Eq. 18 can be written in the form

$$\begin{aligned}G_d&=-\frac{1}{2a_d}\int_{a_d}\left(\sigma_{kl}\left(\mathbf{U}^\tau\right)n_kU_l^0-\sigma_{kl}\left(\mathbf{U}^0\right)n_kU_l^\tau\right)ds=\\&=\underbrace{-\frac{1}{2a_d}\int_{a_d}\left(\sigma_{22}\left(\mathbf{U}^\tau\right)n_2U_2^0-\sigma_{22}\left(\mathbf{U}^0\right)n_2U_2^\tau\right)ds}_{G_{dI}}\underbrace{-\frac{1}{2a_d}\int_{a_d}\left(\sigma_{21}\left(\mathbf{U}^\tau\right)n_2U_1^0-\sigma_{21}\left(\mathbf{U}^0\right)n_2U_1^\tau\right)ds}_{G_{dII}}=\\&\underbrace{\frac{1}{2a_d}\int_0^{a_d}\sigma_{22}\left(\mathbf{U}^0\right)\Delta U_2^\tau ds}_{G_{dI}}+\underbrace{\frac{1}{2a_d}\int_0^{a_d}\sigma_{21}\left(\mathbf{U}^0\right)\Delta U_1^\tau ds}_{G_{dII}}.\end{aligned} \tag{23}$$

On the other side, assume any contour Γ surrounding the crack tip and write

$$G_d = -\frac{1}{2a_d}\int_\Gamma \left(\sigma_{kl}\left(\mathbf{U}^\tau\right) n_k U_l^0 - \sigma_{kl}\left(\mathbf{U}^0\right) n_k U_l^\tau\right) ds = -\frac{1}{2a_d}\int_\Gamma \left(\sigma_{kl}\left(\mathbf{U}^\tau\right) n_k \delta_{lj} U_j^0 - \sigma_{kl}\left(\mathbf{U}^0\right) n_k \delta_{lj} U_j^\tau\right) ds =$$
$$= -\frac{1}{2a_d}\int_\Gamma \left(\sigma_{kl}\left(\mathbf{U}^\tau\right) n_k \left(n_l n_j + t_l t_j\right) U_j^0 - \sigma_{kl}\left(\mathbf{U}^0\right) n_k \left(n_l n_j + t_l t_j\right) U_j^\tau\right) ds =$$
$$= \underbrace{-\frac{1}{2a_d}\int_\Gamma \left(\sigma_{kl}\left(\mathbf{U}^\tau\right) n_k n_l n_j U_j^0 - \sigma_{kl}\left(\mathbf{U}^0\right) n_k n_l n_j U_j^\tau\right) ds}_{G_{dI}} \underbrace{-\frac{1}{2a_d}\int_\Gamma \left(\sigma_{kl}\left(\mathbf{U}^\tau\right) n_k t_l t_j U_j^0 - \sigma_{kl}\left(\mathbf{U}^0\right) n_k t_l t_j U_j^\tau\right) ds}_{G_{dII}}, \tag{24}$$

where t_l is he unit tangential vector of Γ. Thus, the ERR based phase angle ψ_G for deflected crack can be calculated by substituting for G_{dI} and G_{dII} from Eq. 24 to Eq. 22 and making use of Eq. 16.

Note that the ERR and the SIF based measures of mode mixity for an interface crack, phase angle ψ_G and ψ_K, are related by [7]

$$\cos\left(2\psi_G\right) = \sqrt{\frac{\sinh\left(2\pi\varepsilon\right)}{2\pi\varepsilon\left(1+4\varepsilon^2\right)}} \cos\left[2\psi_K + 2\varepsilon \ln\frac{a_d}{2L} + \arg\left[\frac{\Gamma\left(1/2+i\varepsilon\right)}{\Gamma\left(1+i\varepsilon\right)}\right] - \arctan\left(2\varepsilon\right)\right], \tag{25}$$

ε – oscillation index of the interface crack,

with Γ(.) being the gamma function. Eq. (25) can be very useful for evaluation of the fracture energy of the interface $G_{ci}(\psi_K)$ at the mode mixity angle ψ_K. If G_{c2} be the fracture energy of material #1 under the mode I condition, then for $G_{ci}(\psi_K)/G_{c2} > G_d/G_p$, the impinging crack will penetrate across the interface, rather than debond the interface. Otherwise, the impinging crack will debond the interface, rather than penetrate across the interface.

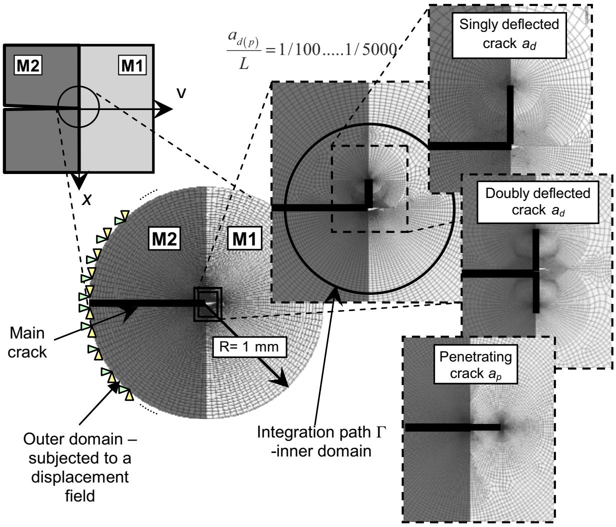

Figure 2. FE mesh for obtaining the $\mathcal{V}_1^h$-FEM approximation to $\mathbf{V}^\tau$, cf. Eq. 12, and $\mathcal{V}_2^h$ – FEM approximation to $\mathbf{V}^\tau$, cf. Eq. 13 in the case of crack perpendicularly impinging the interface. Similar mesh was designed also for inclined cracks.

The orthotropic materials are characterized by two dimensionless elastic parameters λ and ρ $\lambda = s_{11}/s_{22}$, $\rho = (2s_{12} + s_{66})/\sqrt{s_{11}s_{22}}$, where s_{ij} are the material compliances and defined in the conventional fashion. The relative stiffness between the materials M1 and M2 is measured by the two generalized Dundurs parameters α and β [8].

The first step of numerical calculations consists in finding the stronger singularity exponent δ_1, the weaker singularity exponent δ_2, and the corresponding eigenvectors **g** by solving the eigenvalue problem in Eq. 3. In addition to the regular singular solutions also auxiliary solutions are needed for the application of the reciprocal theorem (Ψ-integral) which allows to determine the GSIFs H_1 and H_2 from Eq. 11 and the coefficients $K_{1d(p)}, K_{2d(p)}, K'_{1d(p)}, K'_{2d(p)}$ from Eqs. 12 and 13, see also Fig. 2.

Figure 3 shows the stronger and the weaker singularity exponents as functions of the generalized Dundurs parameters α for the impinging angle ω = 30°, see Fig. 1. Further results concerning the calculations of the ratio of the debonding to the penetrating ERR and the ERR based fracture mode mixity will be presented at the ECF17 meeting.

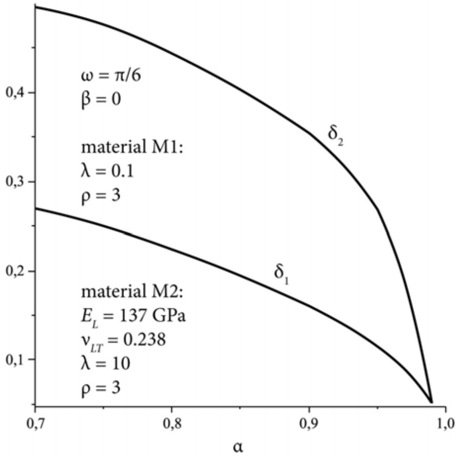

Figure 3. The stronger and the weaker singularity exponents as functions of the generalized Dundurs parameter α for $\beta = 0$, $\omega = 30°$, $\lambda^I = 0.1$, $\lambda^{II} = 10$, $\rho^I = \rho^{II} = 3$, $E_L^{II} = 137\mathrm{GPa}$, $\nu_{LT}^{II} = 0.238$

References

[1] M.Y. He and J.W. Hutchinson: Int J Solids Struct Vol. 25 (1989), p.53.

[2] J. Cook J. and J.E. Gordon: Proc Roy Soc A Vol. 28 (1964), p.28.

[3] D. Leguillon, C. Lacroix and E. Martin: Int. J. Solids and Struct. Vol. 38 (2001), p. 7445.

[4] E.F. Rybicky and M.F. Kanninen: Engn. Fract. Mech. Vol. 9 (1977), p. 931.

[5] Z. Zang and Z. Suo: Int. J. Solids and Struct. Vol. 44 (2007), p. 4559.

[6] J.R. Rice: J. Appl. Mech. Vol. 32 (1988), p.98.

[7] V. Mantic and F. París: Int. J. Fracture Vol. 130 (2004), p.557.

[8] V. Gupta, A.S. Argon and Z. Suo: J. Appl. Mech. Vol 59 (1992), p. S79.

The authors gratefully acknowledge a financial support of the Czech Science Foundation under the projects No. 106/06/0724